JOURNAL OF GEOPHYSICAL RESEARCH, VOL. 85, NO. A7, PAGES 3376-3386, JULY 1, 1980

CORRELATIONS BETWEEN λ4278 OPTICAL EMISSIONS AND VLF WAVE EVENTS OBSERVED AT L ~ 4 IN THE ANTARCTIC

R. A. Helliwell

Radioscience Laboratory, Stanford University, Stanford, California 94305

S. B. Mende

Lockheed Palo Alto Laboratory, Palo Alto, California 94304
J. H. Doolittle, W. C. Armstrong, and D. L. Carpenter
Radioscience Laboratory, Stanford University, Stanford, California 94305

Abstract. One-to-one correlations have been observed at L ~ 4 between bursts of ducted VLF noise in the ~2 to 4-kHz range and optical emissions at λ4278. The optical observations were made at Siple Station, Antarctica, in the austral winter of 1977; the wave activity was recorded both at Siple and its conjugate station Roberval, Canada. The one-to-one correlations were observed during 6 of 32 observing sessions. Most of the events occurred near dawn (prior to interruption of the observations by twilight interference) during or shortly following substorm events (Kp = 2.5; Dst = -10-40). In most of the cases the plasmapause was equatorward of Siple, and the equatorial electron densities were low (~10 cm^{-3}). In one case, July 24, 1977, the equatorial density had recovered to a level of 100 cm^{-3} at the time of observation. The estimated precipitated energy fluxes ranged from 0.04 to 0.1 ergs cm^{-2} s^{-1}. The correlated VLF activity usually consisted of clusters of discrete rising tones or chorus ranging in duration from ~1 s to ~10 s. In three of the six cases some or all of the chorus bursts were triggered by whistlers. Photometer peaks lagged the wave peaks by 1-2 s. In the case of July 24, 1977, a model of the interaction process was constructed using the lag time and the whistler-derived cold plasma density. The data were found to be consistent with scattering of electrons into the loss cone over Siple by emissions that were triggered by waves propagating away from the equator after reflection in the ionosphere over Siple. This interpretation differs from that of a previous study of X-ray bursts induced by similar VLF emissions. This difference is attributed to the occurrence of whistler echoing during the reported X-ray event. During the same period, VLF hiss was observed in the range 2.5-5.0 kHz. Immediately following each discrete event the hiss and the λ4278 intensities were reduced below their pre-event levels for about 10 s. Both reductions are tentatively attributed to a temporary depletion of particles near the loss cone. Recovery to pre-event levels could be explained by refilling of the duct through east-west gradient drift of energetic electrons.

Introduction

A significant transfer of energy from the magnetosphere occurs as energetic particles from the radiation belts precipitate into the ionosphere. When these electrons collide with the ionospheric constituents, they cause enhanced ionization, heating, and the emission of X-rays and light.

One of the causes of such precipitation is electromagnetic waves that scatter particles out of their trapped orbits [e.g., Thorne, 1975]. However, little is yet known about the importance of specific types of waves in particle scattering because of the difficulty in correlating wave events with precipitation events. One reason is that past precipitation studies have been largely confined to the high latitudes of the auroal zone, where precipitation events are too numerous to permit easy identification of the causes. Recent work shows, however, that at mid-latitudes (L ~ 4), isolated bursts of precipitating particles can often be found in association with whistlers and triggered emissions. For example, Rosenberg et al. [1971] found a one-to-one correlation between bursts of whistler-triggered discrete VLF emissions propagating at L ≃ 4.2 and bursts of >30 keV X-rays observed at balloon altitudes. Helliwell et al. [1973] reported a correlation between whistlers and perturbations in VLF propagation in the nighttime earth-ionosphere wave guide. Each perturbation lasted about 30 s and was attributed to whistler-induced precipitation of energetic (30 keV) electrons that created a transient enhancement of thermal electrons in the D region. This enhancement in turn disturbed the phasing of the wave guide modes, causing the observed perturbations. Both the X-ray and VLF propagation anomalies were attributed to cyclotron resonance interaction between energetic electrons and the whistler-mode wave packets in the vicinity of the equatorial plane.

Compared with the X-ray and VLF methods described above, photometric measurements of light emission caused by VLF wave-induced precipitation are capable of providing better spatial resolution of the precipitating particles and should extend the electron energy range to lower values. However, at subauroral latitudes the effects of wave-induced precipitation are difficult to detect. Reasons include the low light levels in precipitation events, uncertainty regarding the location and horizontal extent of the light spot, the intermittent occurrence of events, and the frequent presence of scattered light from the sun, from the moon, and from auroral displays located poleward of the observer.

This paper describes a new mid-latitude experiment in which these difficulties were largely avoided; one-to-one correlations were found be-

Paper number 9A1255.
0148-0227/80/009A-1255$01.00

tween bursts of λ4278 light emissions and quasi-coherent ducted VLF waves. The work is an outgrowth of a program of photometric observations begun in 1974 at Siple Station, Antarctica (76°S, 84°W, L ≃ 4.2) and the conjugate station Roberval, Canada (48°N, 73°W). The present measurements were carried out at Siple Station during the austral winter of 1977.

Theory and experiment have suggested that many types of waves are involved in the magnetospheric particle precipitation process. Recent theoretical work has demonstrated the importance of quasi-coherent waves in the scattering of energetic electrons [Inan et al., 1978]. ELF hiss, an incoherent whistler-mode wave, is believed to play an important role in the control of precipitation of electrons from the mid-latitude magnetosphere at energies above a few 10's of keV [e.g., Lyons et al., 1972]. Coherent signals from high-power VLF transmitters (10-30 kHz) may also cause scattering of such high-energy particles [e.g., Imhof et al., 1978; Vampola and Kuck, 1978]. Particles in the 1 to 20-keV range may be scattered by whistlers, discrete VLF emissions, VLF hiss, and amplified (30 dB) Siple transmitter signals (2-6 kHz) that propagate in the outer plasmasphere. Beyond the plasmapause, coherent signals such as VLF chorus emissions can cause scattering, as documented in the present paper, while broadband noise bursts or bands in the ~2 to 20-kHz range observed just beyond the plasmapause [Carpenter, 1978] may also produce precipitation effects. Another suggested cause of scattering beyond the plasmapause is electrostatic waves [e.g., Ashour-Abdalla and Kennel, 1978], but their relative importance at the Siple latitude has not yet been determined.

Present knowledge regarding electron precipitation fluxes near the plasmapause is summarized as follows:

1. In terms of direct satellite measurements, the average flux at L ~ 4 for E > 40 keV is of the order of 3×10^{-3} ergs cm^{-2} s^{-1} [e.g., Potemra, 1973; Larsen et al., 1976a]. These fluxes are at the lower limit of detection by satellite instruments and are relatively difficult to measure [Larsen et al., 1976a].

2. At mid-latitudes, upper limits of ~10^{-2} ergs cm^{-2} s^{-1} have been inferred by optical methods [e.g., Galperin, 1962; Dalgarno, 1964], in agreement with item 1.

3. Mid-latitude precipitation fluxes appear to be latitude-dependent, generally increasing with latitude [e.g., Larsen et al., 1976b]. The fluxes are also sensitive to the presence of particles injected into the magnetosphere during magnetic disturbances [e.g., Larsen et al., 1976a]. Thus substantially higher flux levels than the ones indicated on items 1 and 2 above are to be expected during substorm activity. As an example, Foster and Rosenberg [1976] inferred precipitation fluxes of the order of 0.1 ergs cm^{-2} s^{-1} during the one-to-one correlations of >30-keV X-ray bursts and VLF chorus activity noted above.

The present study strongly supports item 3 above, showing further that well-correlated optical emissions and discrete VLF noise bursts can frequently be observed outside the plasmapause near 06 MLT.

Description of the Experiment

Optical monitoring of the N_2^+ first negative band gives a very sensitive measure of the energy flux of precipitated particles. A quantitative relationship between the observed column-integrated density of λ4278 emissions and the energy flux of the precipitating electrons is given, for example, by Rees and Luckey [1974]. In the range 1-100 keV, this ratio is 140-210 Rayleigh per erg cm^{-2} s^{-1}, dependent on energy.

The specific instrument used at Siple consisted of a two-channel zenith viewing photometer with a field of view of 10°. A filter of 30-Å width was centered at λ4268 so as to straddle the P and R branches of the first negative N_2^+ λ4278 band. In the second channel a control filter of equal bandwidth centered at λ4300 was provided to confirm the reality of events at λ4278.

In the 1977 Siple field operation, real time identification of correlative activity was emphasized. To aid in reaching this objective, certain modifications of the optical data acquisition system were made. A particularly useful innovation was a voltage-controlled oscillator (VCO), whose frequency depended on the light level. The VCO frequency was recorded on the same audio tape with the broadband VLF signals (see Figures 6 and 7). The light level was also recorded on a digital magnetic tape and on an eight-channel chart displaying a number of geophysical quantities. The chart speed was increased as required (up to 100 mm/min) to improve the time definition of correlated events. A video display of the VLF spectrum was also used to determine the presence of burstlike VLF noises that might be correlated with other geophysical phenomena.

Continuous broadband VLF audio recordings were made of all periods of interest and were bracketed by synoptic recordings which show the character of the VLF activity in nearby periods. The integrated amplitudes of noise in the frequency bands 1-2 kHz and 2-4 kHz were displayed on the chart records for comparison with the photometer analog output. Simultaneous synoptic VLF recordings were made at the conjugate station at Roberval, Quebec.

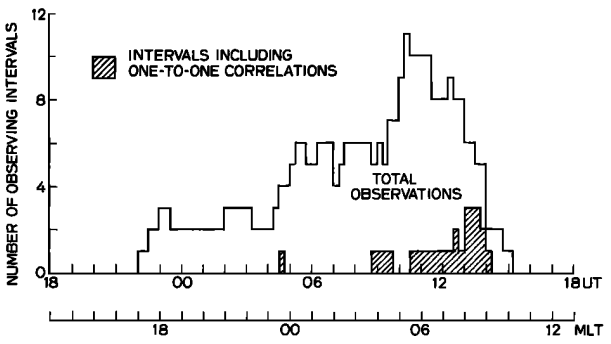

Fig. 1. Histogram of intervals of photometric and VLF observations at Siple Station in 1977. Shading indicates the number of 15-min intervals during which one-to-one correlations were observed.

Observations

There were 32 observing sessions, typically of several hours' duration, in the May-August 1977 period. Six of the sessions include definite one-to-one correlations. Figure 1 shows the distribution of the observations over intervals of 15 min in UT and MLT; the number of intervals containing one-to-one correlations is shown by shading.

During most of the unshaded intervals, amplitude fluctuations above the background level were present (the background level is controlled by sky brightness as well as above the noise level of the instrument). The fluctuations were typically ~5R, and were generally smaller than those observed during the shaded intervals. Occasionally, the burst levels in the unshaded periods equalled or exceeded the levels of the shaded ones. In such cases strong VLF activity was always present, and it is inferred that the correlation was obscured by VLF reception from ducted paths outside the field of view of the Siple photometer. A number of such intervals were classified in the field as 'probable.'

The shape of the histogram of observations depends on several factors. A watch for discrete or burstlike VLF noises was made during many nighttime hours. Attention was somewhat biased toward postmidnight hours, when discrete emission activity such as chorus was expected to build up (the cutoff in observations near 14 UT is due to twilight interference with the photometer). Considerations of opportunity, such as good seeing conditions, and of conflicts, for example, with Siple transmitter schedules, also affected the observing pattern. The successes appear to reflect the predawn buildup in emission activity.

The correlations occurred during periods of moderate disturbance, with Kp in the range 2-5 and Dst in the range -10 to -40. In most of the cases, magnetograms from College, Alaska, showed

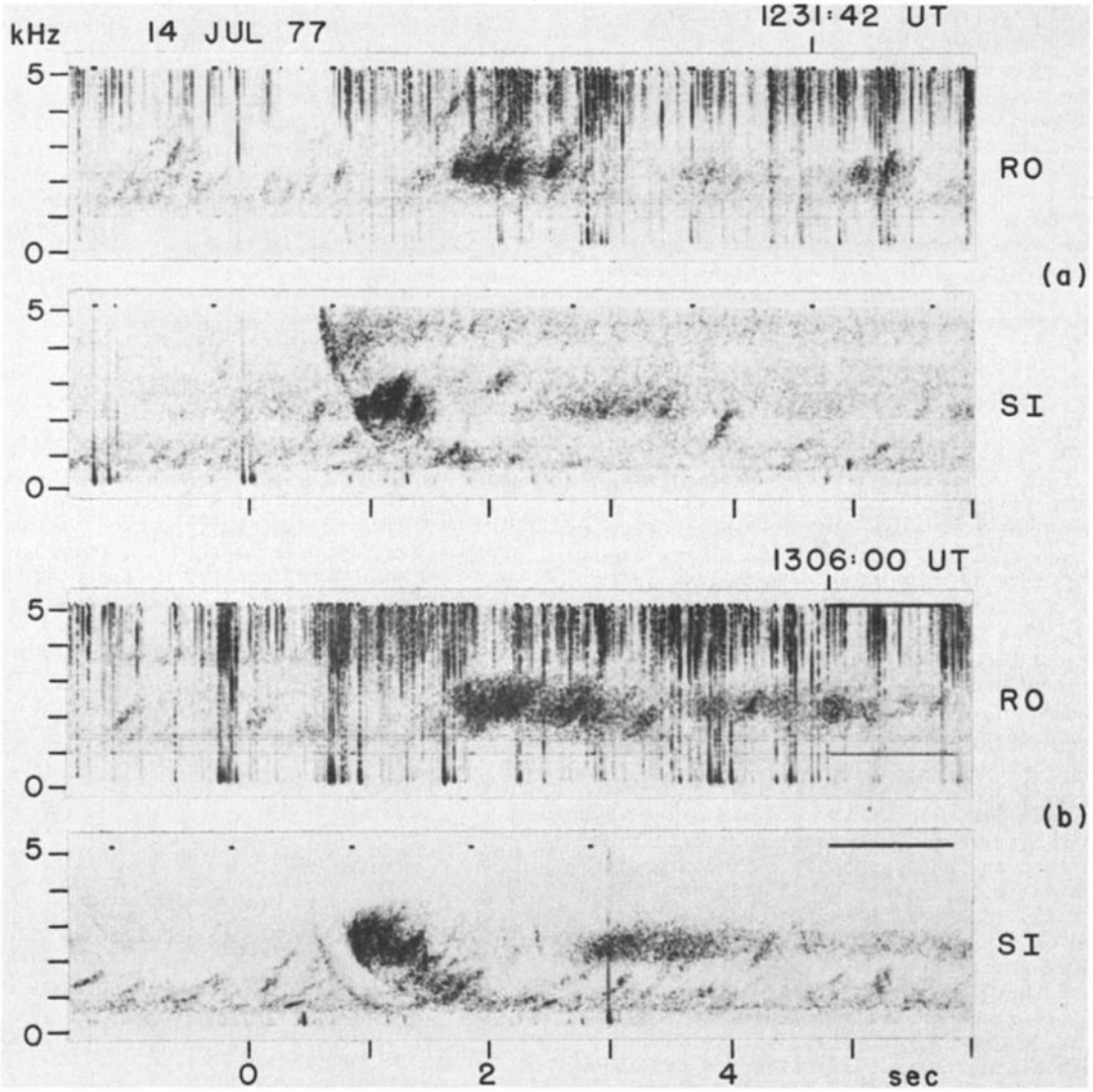

Fig. 2. Spectrographic records from the conjugate stations Roberval and Siple, showing 2-3 kHz VLF noise bursts that were correlated with bursts of λ4278 emissions detected at Siple Station. Two events are displayed, recorded about 30 min apart on July 14, 1977. The correlated noise events appeared first at Siple and were found to have been triggered by whistlers.

substorm activity near local midnight as the event developed near local dawn on the Siple meridian. The general properties of the correlations are summarized as follows:

1. Nature of VLF Events

The correlated VLF activity usually consisted of clusters of discrete rising tones, or chorus. The clusters ranged in duration from ≃1 s to ≃10 s. In one of the six cases (July 24, 1977) all of the correlated wave events involved whistlers and whistler-triggered emissions. In two of the cases (May 17 and July 14, 1977) the stronger chorus events were triggered by identifiable whistlers. Examples of such triggering are shown on spectrograms in Figure 2. The records of the conjugate stations Roberval and Siple are aligned for two events recorded roughly 30 min apart. Inspection of these and other records of the period reveal triggering of noise at ~2-3 kHz by whistler components that have been identified as propagating outside the plasmapause. On the Roberval records, 2 to 3-kHz noise bursts appear following reflection of the waves and their return to the northern hemisphere. A faint third-hop echo is evident at Siple near t = 3 s. Both of the noise events shown were coincident with surges of optical emission activity.

Intensity measurements of the conjugate events of Figure 2 were made at 2.2 kHz. At Siple Station the average received peak intensity of the two one-hop triggered noise bursts was ~2.1 mγ. The corresponding two-hop noise bursts at Roberval averaged 0.35 mγ, a reduction of ~15.6 dB. At this time, Siple was in darkness and Roberval in daylight, so that we would expect more ionospheric absorption of the Roberval signal and hence reduced Roberval strength, just as observed. Allowing a 2-dB loss per hop due to progressive attenuation of the echo train, the net differeince in ionospheric loss is estimated to be 13.6 dB. This is comparable with the predicted differences in typical day and night absorption at 2.2 kHz based on model studies [Helliwell, 1965] . Thus at the top of the ionosphere the field intensity of the northgoing noise burst is predicted to be only 2 dB less than that of the southgoing burst, suggesting that the wave-induced particle scattering should be about the same in the two directions.

An example in which no triggering by whistlers was evident is shown in Figure 3. In this case the VLF activity, shown in parts (b) and (c), consisted of groups of discrete rising tones. In the early part of the record the groups were spaced at intervals of about 10 s.

Irregular spacing of correlated events is illustrated in Figure 4. VLF noise consisted of several-second-long bursts of chorus. Several of the stronger bursts, such as the one at ~0903:35 in Figure 4, showed evidence of triggering by whistlers propagating outside the plasmapause.

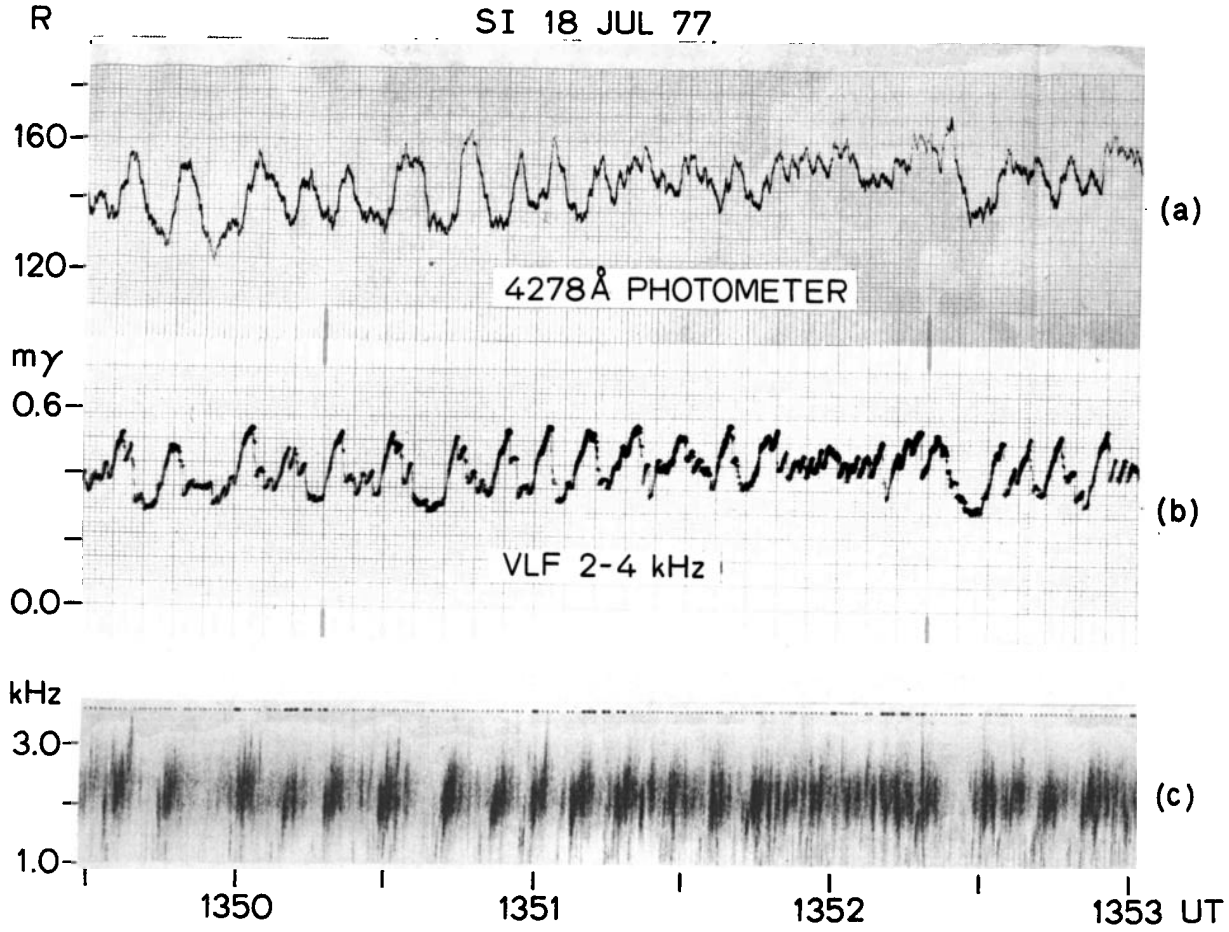

Fig. 3. Charts and spectrographic records from July 18, 1977, showing a high degree of correlation between optical emissions and quasi-periodic bursts of VLF chorus observed at Siple Station.

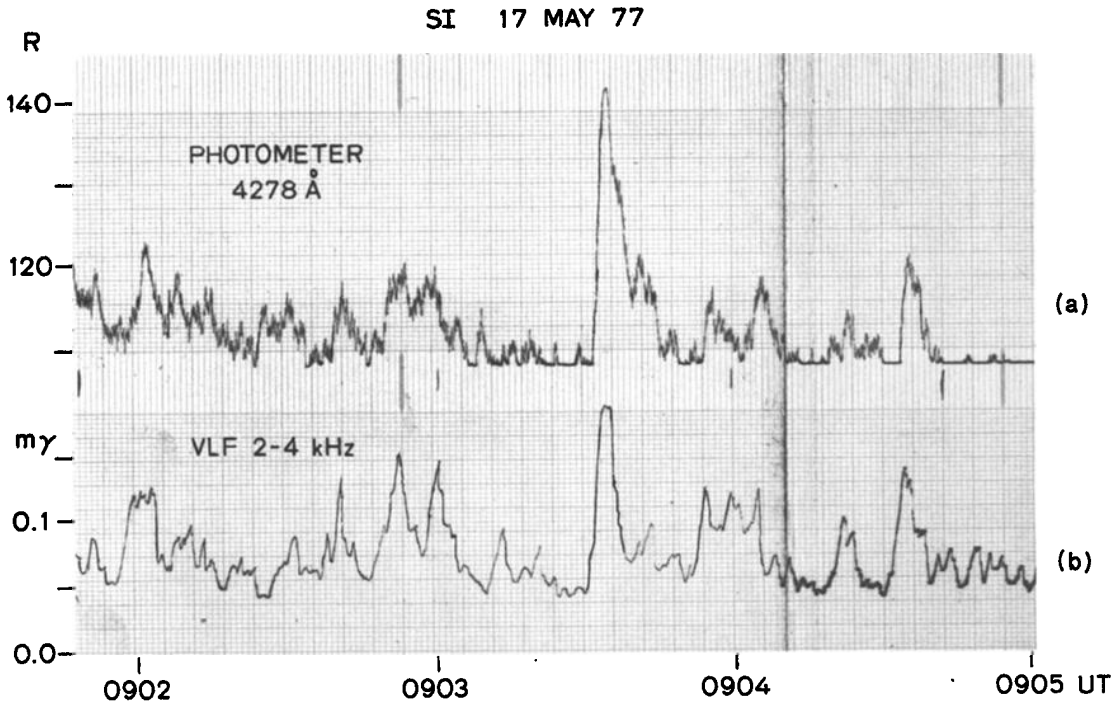

Fig. 4. Charts illustrating a high degree of correlation between optical emissions and VLF activity in the 2 to 4-kHz band observed at Siple Station on May 17, 1977. In this case the VLF consisted of irregularly spaced bursts of chorus, some of which were identified as having been triggered by whistlers.

The extent of triggering of the weaker bursts by whistlers is not known. Because the triggering whistler is usually much weaker than the resulting noise burst (as in Figure 2), the level of the triggering whistler-mode signals propagating outside the plasmapause is frequently below the threshold of detection on spectrographic records. (For additional information on the identification of noise burst triggering by whistlers, see Foster and Rosenberg [1976] and Carpenter [1978].)

Correlation with relatively short (≈1 s) whistler/noise events on July 24, 1977, is illustrated in Figure 5. The outstanding events were marked by arrows in the field as they occurred. The better-defined events occurred at intervals of several minutes. Spectra of the whistler events are shown in Figures 6 and 7 and are discussed further below.

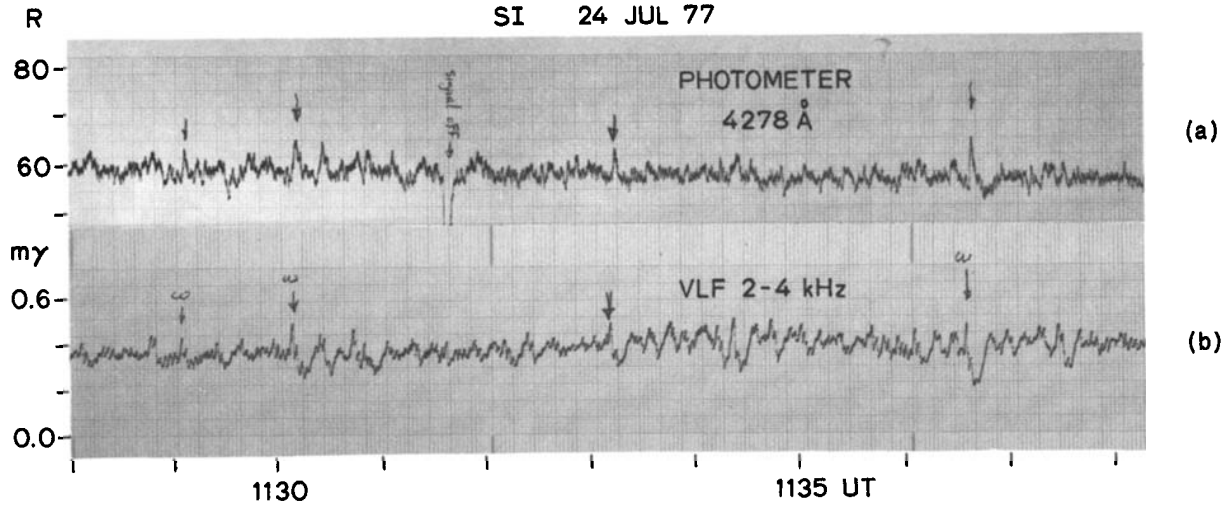

Fig. 5. Chart records from July 24, 1977, illustrating one-to-one correlations (arrows) between optical emissions and VLF activity in the 2 to 4-kHz band. Each of the VLF events involved a well-defined whistler and burst of triggered VLF chorus. Peak amplitudes of sudden VLF events are somewhat reduced due to 1 second integration which is intended to eliminate impulsive noise.

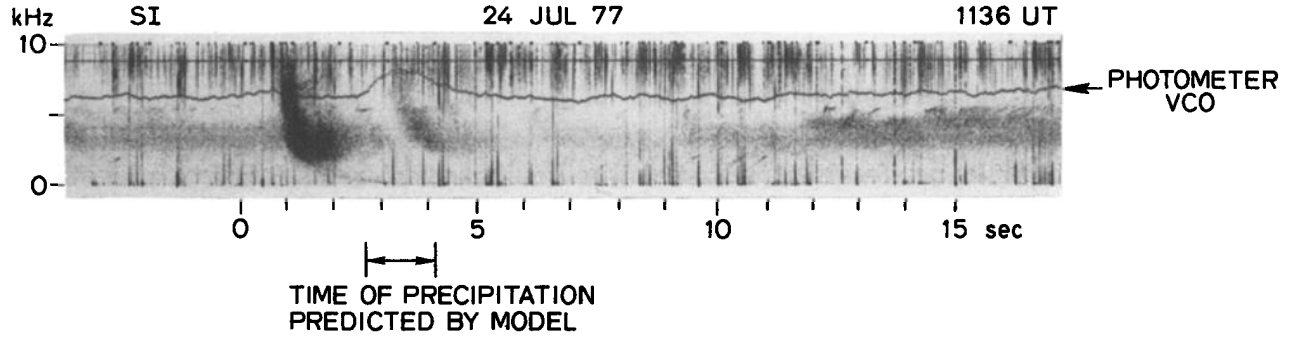

Fig. 6. Spectrographic record from July 24, 1977, illustrating a whistler received at Siple Station and a correlated photometric event. The time scale is referenced to the occurrence of the causative atmospheric. Suppression of a diffuse band of noise near 3 kHz occurs for about 10 s following the whistler. The horizontal bar beneath the record indicates an estimate of the time of occurrence of optical emissions, based on an interpretive model discussed in a later section.

2. Variations in Correlation

In five of the six cases, one-to-one correlations were observed over intervals of 1 to 2 hours. In most cases, the peak-to-peak relation between large VLF and optical bursts persisted throughout the period, while the degree of correlation at lower burst amplitudes varied on a time scale of ~2 to 10 min. Figures 3 and 4 illustrate intervals of several minutes' duration in which there appeared to be a high degree of correlation over a wide range of amplitude levels. In contrast, Figure 5 shows an apparently low degree of correlation during several of the intervals separating the large, well-correlated peaks. Reduced correlation at lower amplitudes may in some cases be due to interference from noise bursts associated with precipitation regions that were outside the field of view of the Siple photometer.

3. Path Properties, Plasmapause Position, Electron Density, and Approximate Resonant Energies

Whistler analysis [e.g., Park, 1972; Seely, 1977] was applied in five of the six cases (the August 8 case involved a single isolated VLF burst that was not recorded on magnetic tape). In four of the six cases the correlated waves were identified as propagating ~0.5-1.5L beyond the plasmapause. In one case, that of July 24, 1977, propagation occurred within a region of irregular density variation, and a plasmapause was not defined in the data.

In cases of one-to-one correlation with a zenith-looking photometer it is assumed that the interacting waves propagate on field lines that pass near the observing station. To test this assumption, the positions of magnetospheric wave path endpoints at 100-km altitude with respect to Siple were estimated by a combination of whistler dispersion measurements and mapping along field lines using a hybrid Olson-Pfitzer/IGRF geomagnetic field model [Seely, 1977]. Use of such a model is important; near Siple its endpoint predictions differ from those of a dipole model by as much as 200 km in the north-south direction [Seely, 1977]. In three of the four cases of identifiable triggering by whistlers the analysis was consistent with VLF propagation on field lines nearly overhead at Siple, within a radius of 100 km. In the fourth case the estimated path endpoint was ~200 km poleward of the station. However, this and the other cases remain subject to propagation and field-model uncertainties that are estimated to be of the order of 100 km.

In cases of propagation beyond the plasmapause the equatorial electron density along the VLF paths was of the order of 10 el cm^{-3}. For cyclotron resonant scattering by waves in the approximately 2 to 4-kHz range within $\pm \sim 20°$ of the magnetic equator this corresponds to parallel particle energies in the range ~10-300 keV. In the case of July 24 the electron density level at ~4.2R_E was about 100 el cm^{-3}, intermediate between typical plasmasphere and plasmatrough levels. The corresponding parallel resonant energies, discussed in later paragraphs, were between 1 and 30 keV.

4. Time Lag

The photometer peaks lagged the peaks in wave activity by intervals ranging from ~1 to 2 s. The measured lag in the case of Figure 3 was about 1.2 s. Figure 6 shows the lag by means of a photometer VCO injected in the 6 to 9-kHz range of the VLF spectrum. The light pulse that begins at about 2.6 s is centered approximately 2 s following the main body of the whistler and its associated emission.

5. Hiss Correlation

An apparent connection between a diffuse hiss-like noise background and the optical emission level was observed on July 24, 1977, as shown in Figures 6 and 7. The hiss and the light level were both reduced immediately following discrete wave events and their correlated optical bursts. Figure 6 shows such an event near 1136; Figure 7 repeats this event and compares it to a series of other events recorded over a period of about 50 minutes. Prior to each whistler event, a diffuse noise band was present between ~2.5 and 5.0 kHz. Immediately following the whistler event, the hiss level was reduced by ~4-6 dB and then recovered over a period of about 10 s, as illustrated in Figure 6. Similar behavior was observed in the conjugate point record (not shown). The same event is also shown at the right-hand arrow in Figure 5 (in this case, the 1-s inte-

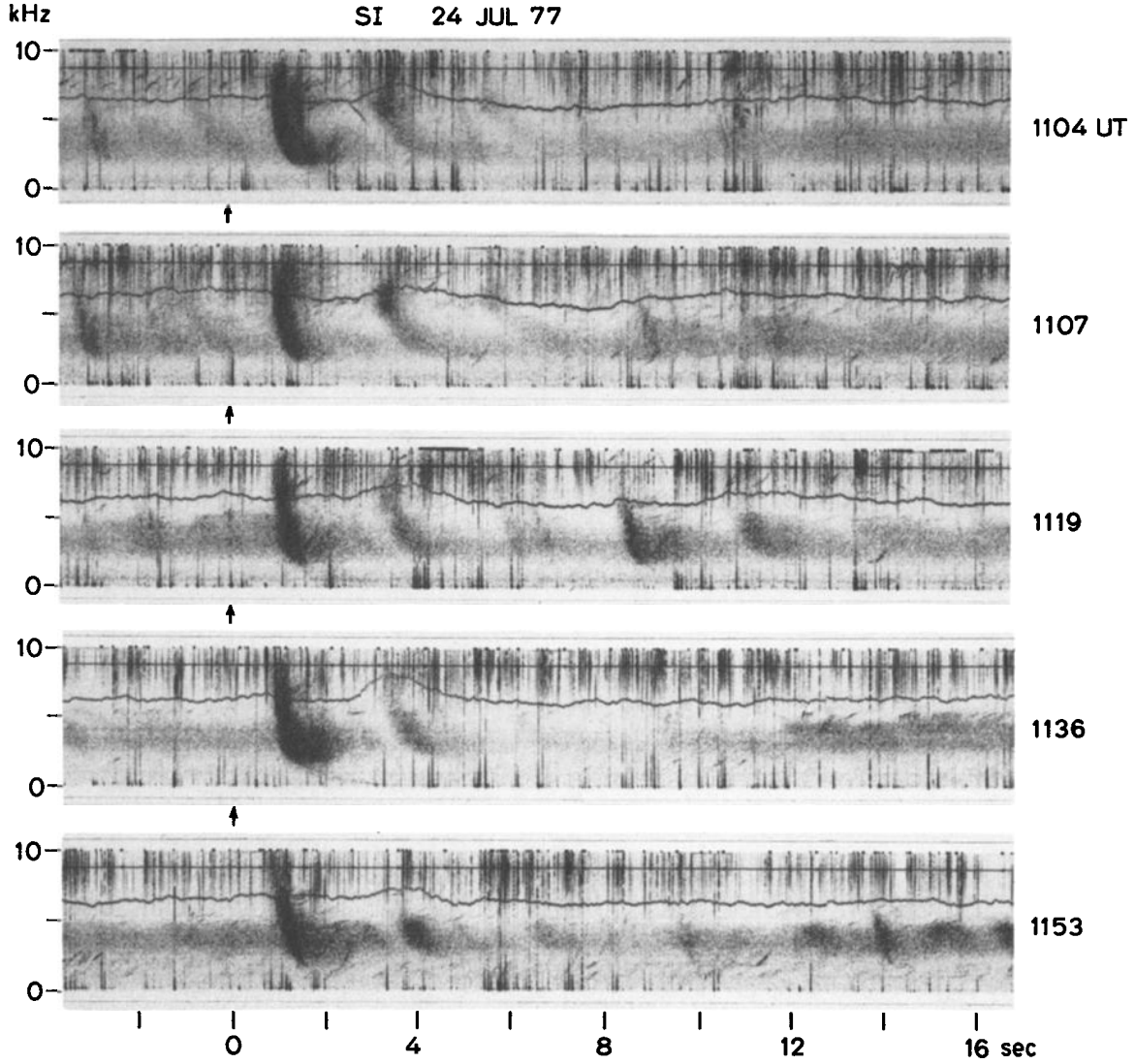

Fig. 7. Spectrographic records of whistlers that were correlated with increases in optical emissions at Siple Station. The recordings cover an interval of approximately 1 hour on July 24, 1977. The times marked at the right correspond to the beginning of the 1-minute interval containing the event. The time scales are aligned with respect to the time of occurrence of the causative atmospherics.

gration used in the filtering reduced the apparent amplitude of the whistler event).

The chart of Figure 5 shows that between 1136 and 1137 UT there was a postevent reduction in photometer output as well as in 2 to 4-kHz noise. Slow variations of this kind are not apparent in the VCO traces of Figures 6 and 7, since the VCO display is logarithmic and self-zeroing.

6. Inferred Energy Fluxes of Precipitating Electrons

The photometric bursts tended to range from ~10 to 30 R above background. From the calculation of Rees and Luckey [1974] this corresponds to energy fluxes of 1 to 100-keV electrons in the range ~0.04-0.10 erg cm^{-2} s^{-1}.

S3-3 satellite particle measurements were made on July 24, 1977, in the northern hemisphere at ~2100-km altitude (courtesy of R. Sharp). The satellite was roughly conjugate to Siple, passing ~12° west of Roberval at 1312 UT, within ~30 min following the period of correlated observations at Siple. The total electron energy flux was approximately 2.5×10^7 keV cm^{-2} s^{-1} sr^{-1}; most of the energy was in the range 7.2-24 keV. The fluxes were isotropic outside the upward loss cone, so that the inferred precipitating flux was $\sim 8 \times 10^7$ keV cm^{-2} s^{-1} or 0.1 erg cm^{-2} s^{-1}.

While this flux cannot be compared directly with the burstlike Siple observations, it suggests that quasi-steady precipitation at a level comparable to the burst amplitudes was present near the Siple latitude. The presence of a quasi-steady component of precipitation in the July 24 case is suggested by the postevent reduction in photometric output noted just above (also see next section).

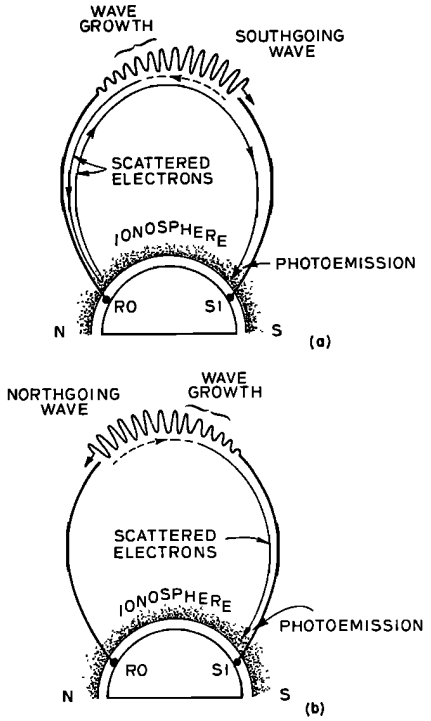

Fig. 8. Diagrams showing two possible models of the interactions leading to the one-to-one correlations of July 24, 1977: (a) an interaction involving waves moving southward from a northern hemisphere whistler source; (b) an interaction involving waves moving northward following reflection at the southern hemisphere end of the path.

Interpretation

Because of the close similarity between these results and those of the X-ray and VLF propagation experiments mentioned earlier, we have assumed cyclotron resonance to be the cause of the inferred electron scattering. Energetic electrons interact with whistler-mode waves traveling in the opposite direction through the mechanism of Doppler-shifted cyclotron resonance. This interaction may transfer energy either to or from the wave. In either case the interacting electrons are scattered in pitch angle by amounts that depend on wave intensity. Some of these electrons are precipitated into the ionosphere where they produce X-rays, enhanced ionization, and auroral emissions. This interaction often causes growth of narrowband (quasi-coherent) waves of as much as 30 dB [Stiles and Helliwell, 1977]. The growth region is thought to lie near the equatorial plane [Helliwell, 1967].

We can estimate the equatorial wave intensity at the output of the growth region assuming no losses between the equatorial plane and the top of the ionosphere. Taking L = 4.2, the deduced value of equatorial density of 100 el cm^{-3}, and a frequency of 3.5 kHz, we obtain a refractive indes of 16. Thus the magnetic field intensity will be increased by $\sqrt{16}$ from the subionospheric level of ~2 mγ (discussed above) to 8 mγ because of the impedance change. This value is close to the 10-mγ field required by Inan et al. [1978] to produce 0.1 ergs cm^{-2} s^{-1} of precipitation under a representative set of conditions at L = 4.

The ground-observed signals associated with photometer pulses were often weaker than 1 mγ. This does not necessarily imply lower fields in the equatorial plane. The reason is that scattering and refraction effects in the ionosphere are likely to reduce the amount of downcoming wave energy that can enter the transmission cone [Helliwell, 1965] and hence reach the ground.

On the basis of cyclotron resonance we suggest two alternative interaction models of the particle scattering process, as illustrated in Figure 8. In each case the waves originate in a lightning discharge near Roberval (RO) and the light pulse comes from the ionosphere over Siple (SI). In case a the whistler is amplified and emissions are triggered as a 'southgoing' wave moves through a disturbed interaction region near the equator. As the amplified wave moves past the equator, it resonates with 'northgoing' electrons, some of which are scattered into the Roberval loss cone, presumably giving rise to a light pulse (not measured in this experiment). Since the mirror altitude over Siple is less than that over Roberval [Barish and Wiley, 1970], some electrons just outside the Roberval loss cone would reflect back and enter the Siple loss cone. Others will enter the Siple loss cone through scattering in the atmosphere over Roberval, estimated to be about 10% of the incident flux [Davidson and Walt, 1977]. Thus the time delay of the precipitating electrons with respect to the source discharge would be roughly the sum of one-half of a wave hop and one-and-a-half electron hops. This was the model employed to explain the whistler-triggered X-ray bursts of Rosenberg et al. [1971].

In case b the whistler and associated emissions are reflected at Siple and then are amplified and trigger new emissions as they travel northward across the equator. As these strong northgoing waves leave the equator, they scatter southgoing electrons directly into the Siple loss cone. The precipitation time delay is then approximately one-and-a-half wave hops plus a half electron hop.

To test these models, we compute in each case the expected arrival times for comparison with the observations. It is important to allow the interaction region to deviate from the equator in accordance with the resonance requirements. The necessary basic relations for the particle parallel resonant velocity and wave group velocity are [e.g., Helliwell, 1965]

$$v_{\parallel r} = c \frac{(f_H - f)^{3/2}}{f_o f^{1/2}} \quad (1)$$

and

$$v_g = 2c \frac{f(f_H - f)^{3/2}}{f_o f_H} \quad (2)$$

respectively, where

f = wave frequency, kHz;
$f_o = 9\sqrt{N}$, plasma frequency, kHz;
N = electron concentration, cm^{-3};
f_H = electron gyrofrequency, kHz;
c = velocity of light.

Electron travel time from equator to ionosphere is given by [Hamlin et al., 1961]

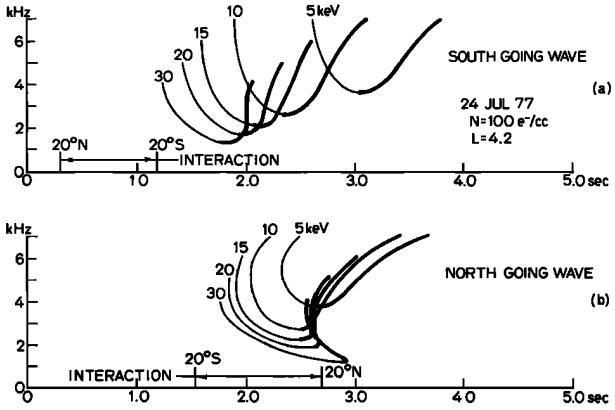

Fig. 9. Predicted arrival time over Siple Station of electrons undergoing interactions with waves of specific frequencies in the 1 to 7-kHz range. Time is measured from the origin in the northern hemisphere of the waves indicated schematically in Figure 8. (a) The results for the southgoing wave of Figure 8a. The time during which the waves move between ±20° of the equator and thus intersect strongly with the magnetospheric particles is indicated along the time scale. Preferential scattering of electrons which are upstream of the equator is shown by extra heavy curves. (b) Similar results for the northgoing wave described in Figure 8b.

$$t_{eq} = \frac{R_{eq}}{v_{\parallel r}} \cdot H(\mu) \qquad (3)$$

where R_{eq} is the geocentric distance to equatorial crossing, $H(\mu) \approx 1.30-0.56\mu$, $\mu = \sin^4\theta_t$, and θ_t is the colatitude of mirror point.

When the interaction region is not on the equator we correct the particle travel time by simply adding $S/v_{\parallel r}$ to (3), where S is the upstream distance of the interaction region from the equator. The use of $v_{\parallel r}$ is justified by the fact that we are interested only in pitch angles less than the loss cone angle (~5°) and hence the total velocity $v \approx v_{\parallel r}$ throughout the assumed interaction region (±20° around the equator).

An approximate correction for the wave travel time is made by applying (2) to small segments of the path between the equator and the interaction region and adding the resulting delay to the one-half hop travel time measured from the triggering whistlers. Note that both corrections are in the same sense.

Numerical calculations based on the above model were carried out for a set of observations on July 24, 1977, for which a path model could be derived from the whistlers. In this case $N_{eq} = 100$ cm^{-3} at $R_{eq} = 4.2R_E$. A diffusive equilibrium model of electron distribution is assumed, in which the concentration is roughly constant throughout the ±20° interaction region [Angerami and Carpenter, 1966; Park, 1972]. A dipole magnetic field model was used, although for the mapping purposes described earlier a realistic geomagnetic model [Seely, 1977] was employed. The whistler one-hop delay at the nose frequency of 4.1 kHz is 1.21 s and increases slightly at higher and lower frequencies. The parallel resonant electron energy is found by substituting (1) in the expression

$$E_k = m_o c^2 \left(\frac{1}{\sqrt{1 - \left(\frac{v_\parallel}{c}\right)^2}} - 1 \right) \qquad (4)$$

where m_o is the rest mass of an electron.

Curves of interacting wave frequency versus time of arrival for electrons of different energies for the two models of Figure 8 are shown in Figure 9. The curves for the upstream side of the equator (see Figure 8) are shown with extra heavy lines. It is at once apparent from the curves for the northgoing wave (Figure 9b) that on the upstream side of the equator there is a focusing effect on the time delay with respect to energy. Thus all electrons in the energy range 10-25 keV and the frequency range 3-4 kHz arrive at Siple within a time interval of only 200 ms, assuming a short VLF wave train. At 3.0 kHz this duration is less than 100 ms. This interesting circumstance is explained by the fact that as the region of interaction moves away from the equator the energy of resonance for a given frequency increases because f_H is rising (see equation (1)). Thus the particle speed increases, partly compensating for the increases in the lengths of both the wave path and the particle path; the result is a kind of time delay 'focusing.' Such an effect may explain microburst phenomena in which short bursts of precipitating electrons are seen over a wide energy range [e.g., Parks, 1979].

Since Figure 9 gives only the onset of precipitation, we must extend the indicated times by the length of the observed wave train. From Figure 6 we estimate the length of the wave train (whistlers at L = 4.2 plus triggered emissions) to be about 1.2 s in the 2 to 5-kHz range. Adding this interval to the times given by Figure 9, we see that for interaction on the upstream side of the equator the southgoing and the northgoing wave trains produce precipitation over the time intervals 2.0 to 4.8 s and 2.6 to 4.2 s, respectively. The observed photometer pulse occupies the interval 2.6 to 4.3 s and therefore is in better agreement with the northgoing wave model. If the downstream sides of the equator were included as scattering regions, the onset times would be advanced roughly 0.6 s in both cases, in disagreement with the observations. This fact supports the assumption that significant scattering is confined to the upstream sides of the equator.

In contrast to the January 2, 1971, X-ray event [Rosenberg et al., 1971], good echoing such as that illustrated in Figure 2 was observed on this day. As was mentioned earlier, the two-hop wave packet seen at RO is estimated to be only 2 dB weaker than the one-hop signals seen at Siple. Since in this case no backscattering is required to account for the precipitation, we conclude that Figure 8b is the more plausible model. (To test this prediction light measurements are being made at both Siple and Roberval.)

The observed 6-dB reduction in hiss amplitude in the ~8-s period following the photometer pulse might be explained as follows. Consider the equatorial region of the duct in which coherent emissions are being triggered by whistlers, and assume that incoherent hiss is generated there through the electron whistler-mode interaction [Kennel and Petschek, 1966]. Such hiss generation is self-limiting because of its dependence

on the anisotropy in the electron pitch angle distribution caused by precipitation. An increase in the anisotropy intensifies the hiss, making the incoherent waves more effective in scattering electrons through cyclotron resonance. As electrons are scattered into the loss cone, the anisotropy and hiss generation are reduced. To sustain a balance, the loss of electrons by precipitation must be equalled by a gain due to west-east gradient drift and flow perpendicular to the electric field. Wave attenuation in the medium is assumed to be less than the intensity gain due to hiss generation.

Precipitation resulting from hiss generation would occur as a quasi-constant 'drizzle' which could have contributed to the background level of optical emissions seen prior to the whistler-correlated light burst (Figure 5). The burst itself results from a much more effective scattering by the very intense whistler and emissions which momentarily fill the loss cone and reduce the hiss generating instability. A simultaneous reduction in the background level of optical emissions can be attributed to the absence of hiss as a scattering wave. The recovery of the hiss and associated drizzle occurs as the anisotropy is restored by precipitation, diffusion, and electron drift. The time required for restoration of the pitch angle distribution due to gradient drift has been inferred from other observations to be of the order of 20 s [Raghuram, 1977], in reasonable agreement with the photometric observations.

An alternative explanation for the hiss reduction is enhanced VLF absorption caused by the precipitation. Thus if the inferred precipitating fluxes of about 0.1 ergs cm^{-2} s^{-1} were present over the full field of view (~200-km diameter) of the Siple 30-MHz riometer, then from the calculations of Bailey [1968], as reported by Rosenberg and Barcus [1978], it is predicted that riometer absorption events of about 0.75 dB should occur. However, if the precipitation is confined to the cross-sectional area of a typical whistler duct (~30-km diameter), then the effect on the riometer could be as much as 30 dB smaller. At Siple, fluctuations above the riometer analog chart noise level of ~0.1 dB were not observed during the periods of correlated optical and wave bursts. Thus it is possible for a small region of absorption to exist in the ionosphere below the duct, sufficient to cause the observed attenuation of a field-aligned hiss signal, but not large enough in area to interfere with the detection of cosmic noise by the riometer.

The model used to determine the arrival times of various energy electrons at Siple has also been used to determine arrival times at Roberval. A similar focusing in arrival times occurs at Roberval about 1.3 seconds after the causative atmospheric. If the reduction of the VLF hiss was due to increased ionospheric absorption, then it should begin at that time. Conjugate VLF records exist for just one correlation event on July 24, 1977 (1150:08 UT), because Roberval recordings were made only at synoptic intervals. Both Siple and Roberval show strong VLF hiss that begins to fall in amplitude about 3 seconds after the atmospheric. Both hiss signals reach a minimum of 4 dB below the intitial intensity about 8 seconds after the atmospheric, then recover in the next 7 seconds. The absence of an absorption effect at Roberval 1.3 seconds after the atmospheric and the conjugate concurrence of the hiss reductions suggests that the source suppression hypothesis offers a better explanation.

Discussion

We are only in the beginning stages of this work. We must measure the size, position and dynamics of the regions of optical and correlated wave activity, the properties of the precipitating particles, and the intensity of the waves in the interaction region. Optical measurements at a number of key wavelengths can provide useful information on the type and energy of the particles. Such diagnostic techniques have been used extensively by a number of groups since their introduction [Eather and Mende, 1971]. The ratio of λ6300 OI to the precipitated energy or the N_2^+ emission may be used to obtain the mean depth of penetration and the energy associated with the precipitating electrons. This technique would be valuable in defining the energy of the λ4278 pulses that are correlated with the VLF wavebursts.

Because of the long lifetime of the parent state of the λ6300 OI emission, the energy measurement can only be obtained on an average basis, and one cannot measure the mean energy of precipitation in a single pulse. Nevertheless, the average energy of precipitation, especially as it is mapped in two dimensions above the VLF-optical ground site, will facilitate interpretation of the spatial relationship between VLF-correlated optical emissions and the more general patterns of nearby precipitation activity.

We conclude that VLF-wave-induced precipitation can be reliably measured using photometer techniques. This should lead to greatly improved accuracy in the measurement of the location and size of precipitation 'spots.' Low-light-level TV may ultimately give a dynamic view of such precipitation. We have also further confirmed a model of scattering by cyclotron resonance in the equatorial region. A new finding is the reduction of hiss and light intensity following correlated wave and optical bursts; its study should lead to improved understanding of the interaction process.

Acknowledgments. We wish to thank J. P. Katsufrakis for his excellent management of Stanford field station operations, John Billey for his assistance at Roberval Station, Peter Harding, Jim Logan, and Ron Marsh for winter-over support at Siple Station, Jerry Yarbrough and Beth Blockley for assistance in data handling and processing, and Gabrielle Daniels and Kris Dean for assistance in preparing the typescripts.

The work at Stanford was supported in part by the National Science Foundation, Division of Polar Programs, under grants DPP74-04093 and DPP76-82646, and by the Office of Atmospheric Sciences Section of the National Science Foundation under grant ATM78-05746. Work at Lockheed was supported by the Division of Polar Programs of the National Science Foundation under grant DPP71-01668.

The Editor thanks J. C. Foster and R. M. Thorne for their assistance in evaluating this paper.

References

Angerami, J. J., and D. L. Carpenter, Whistler studies of the plasmapause in the magnetosphere, 2: Equatorial density and total tube electron content near the knee in magnetospheric ionization, J. Geophys. Res., 71, 711, 1966.

Ashour-Abdalla, M., and C. F. Kennel, Nonconvective and convective electron cyclotron harmonic instabilities, J. Geophys. Res., 83, 1531, 1978.

Bailey, D. K., Some quantitative aspects of electron precipitation in and near the auroral zone, Rev. Geophys. Space Phys., 6, 289, 1968.

Barish, F. D., and R. E. Wiley, World contours of conjugate mirror locations, J. Geophys. Res., 75, 6342, 1970.

Carpenter, D. L., Whistlers and VLF noises propagating just outside the plasmapause, J. Geophys. Res., 83, 45, 1978.

Dalgarno, A., Corpuscular radiation in the upper atmosphere, Ann. Geophys., 20, 65, 1964.

Davidson, G., and M. Walt, Loss cone distributions of radiation belt electrons, J. Geophys. Res., 82, 48, 1977.

Eather, R. H., and S. B. Mende, Systematics in auroral spectra, J. Geophys. Res., 77, 660, 1972.

Foster, J. C., and T. J. Rosenberg, Electron precipitation and VLF emissions associated with cyclotron resonance interactions near the plasmapause, J. Geophys. Res., 81, 2183, 1976.

Galperin, Y. I., The energy sources of the upper atmosphere, Bull. Acad. Sci. USSR, Geophys. Ser., Engl. Transl., 2, 174, 1962.

Hamlin, D. A., R. Karplus, R. C. Vik, and K. M. Watson, Mirror an azimuthal drift frequencies for geomagnetically trapped particles, J. Geophys. Res., 66, 1, 1961.

Helliwell, R. A., Whistlers and Related Ionospheric Phenomena, Stanford University Press, Stanford, Calif., 1965.

Helliwell, R. A., A theory of discrete VLF emissions from the magnetosphere, J. Geophys. Res., 72, 4773, 1967.

Helliwell, R. A., J. P. Katsufrakis, and M. L. Trimpi, Whistler-induced amplitude perturbation in VLF propagation, J. Geophys. Res., 78, 4679, 1973.

Imhof, W. L., J. B. Reagan, and E. E. Gains, The energy selective precipitation of inner zone electrons, J. Geophys. Res., 83, 4245, 1978.

Inan, U. S., T. F. Bell, and R. A. Helliwell, Nonlinear pitch angle scattering of energetic electrons by coherent VLF waves in the magnetosphere, J. Geophys. Res., 83, 3235, 1978.

Kennel, C. F., and H. E. Petschek, Limit on stably trapped particle fluxes, J. Geophys. Res., 71, 1, 1966.

Larsen, T. R., J. B. Reagan, W. L. Imhof, L. E. Montbriand, and J. S. Belrose, A coordinated study of energetic electron precipitation and D-region electron concentrations over Ottawa during disturbed conditions, J. Geophys. Res., 81, 2200, 1976a.

Larsen, T. R., W. L. Imhof, and J. B. Reagan, L-dependent energetic electron precipitation and mid-latitude D-region pair production profiles, J. Geophys. Res., 81, 3444, 1976b.

Lyons, L. R., R. M. Thorne, and C. F. Kennel, Pitch-angle diffusion of radiation belt electrons within the plasmasphere, J. Geophys. Res., 77, 3455, 1972.

Park, C. G., Methods of determining electron concentrations in the magnetosphere from nose whistlers, Tech. Rep. 3454-1, Stanford Electron. Lab., Stanford Univ., Stanford, Calif., 1972.

Parks, G. K., Microburst precipitation phenomena, paper presented at Annual Conference Int. Ass. of Geomagn. and Aeron. and Int. Ass. of Meteorol. and Atmos. Phys., Seattle, Sept. 3, 1977.

Parks, G. K., Microburst precipitation phenomena, J. Geomagn. Geoelec. (in press), 1979.

Potemra, T. A., Precipitating energetic electrons in the midlatitude lower ionosphere, in Physics and Chemistry of Upper Atmospheres, vol. 67, D. Reidel, Hingham, Mass., 1973.

Raghuram, R., Suppression effects associated with VLF transmitter signals injected into the magnetosphere, Tech. Rep. 3456-3, Stanford Electron. Lab., Stanford Univ., Stanford, Calif., 1977.

Rees, M. H., and D. Luckey, Auroral electron energy derived from ratio of spectroscopic emissions, 1: Model computations, J. Geophys. Res., 79, 5181, 1974.

Rosenberg, T. J., R. A. Helliwell, and J. P. Katsufrakis, Electron precipitation associated with discrete very-low-frequency emissions, J. Geophys. Res., 76, 8445, 1971.

Rosenberg, T. J., and J. R. Barcus, Energetic particle precipitation from the magnetosphere, in Upper Atmosphere Research in Antarctica, Antarctic Res. Ser., vol. 29, edited by L. J. Lanzerotti and C. G. Park, AGU, Washington, D. C., 1978.

Seely, N. T., Whistler propagation in a distorted quiet-time model magnetosphere, Tech. Rep. 3472-1, Stanford Electron. Lab., Stanford Univ., Stanford, Calif., 1977.

Stiles, G. S., and R. A. Helliwell, Stimulated growth of coherent VLF waves in the magnetosphere, J. Geophys. Res., 82, 523, 1977.

Thorne, R. M., Wave-particle interactions in the magnetosphere and ionosphere, Rev. Geophys. Space Phys., 13, 291, 1975.

Vampola, A. L., and G. L. Kuck, Induced precipitation of inner zone electrons, 1: Observations, J. Geophys. Res., 82, 2543, 1978.

(Received March 14, 1979;
revised August 8, 1979;
accepted August 21, 1979.)